Grzegorz MIECZKOWSKI

CRITERION FOR CRACK INITIATION FROM NOTCH LOCATED AT THE INTERFACE OF BI-MATERIAL STRUCTURE

KRYTERIUM PĘKANIA STRUKTURY BI-MATERIAŁOWEJ Z OSTRYM KARBEM USYTUOWANYM NA INTERFEJSIE*

The fracture process of bi-material structure with the notch was analysed in this work. For fracture prediction, a criterion based on the Theory of Critical Distances was used. Under analysis were elements made of aluminium alloy and polymer combination (with a various structural notch-tip angle), which then were subjected to the three-point bending test. Values of critical loads resulting from the used hypothesis were compared with values obtained from the experiment. Validation of the selected criterion required defining a qualitative and quantitative description of singular stress fields present around the structural notch-tip area. Therefore, such solutions were obtained and methodology of their determining was discussed.

Keywords: *crack initiation, interface fracture, bi-materials, singular stress fields, stress intensity factors.*

W pracy przedstawiono wyniki badań dotyczących pękania struktury bi-materiałowej z karbem usytuowanym na interfejsie. Do prognozowania inicjacji procesu pękania zastosowano kryterium oparte na punktowej teorii krytycznych dystansów. Analizowano elementy wykonane ze stopu aluminium i polimerów (PC, PMMA), które poddane były trójpunktowemu zginaniu. Wartości obciążeń krytycznych wynikających z wykorzystanej hipotezy porównano z wartościami uzyskanymi z eksperymentu. Walidacja wybranego kryterium wymagała określania jakościowego i ilościowego opisu osobliwych pól naprężeń, występujących w okolicy wierzchołkowej karbu strukturalnego. W związku z tym, uzyskano takie rozwiązania i omówiono metodykę ich otrzymywania.

Słowa kluczowe: *inicjacja procesu pękania, bi-materiały, osobliwe pola naprężeń, współczynniki intensywności naprężeń.*

1. Introduction

Predicting durability of mechanical structures is a complex process that requires many factors to be taken into account. One of them is a structural complexity of structures. The structure is a physical object consisting of many elements, frequently made of materials with different mechanical and physical properties. Additionally, structures are usually subject to complex external loads, frequently of variable nature to various environmental factors. This results in various damage mechanisms – wear (corrosive, cavitational, frictional), fracture – often eliminating a device from further operation.

A point of initiation of cracks, in most cases, are voids and other material defects, and structural notches, the presence of which in the structure most often results from the necessity to join individual components to each other, providing the structure with the required feature characteristics, or requested material structure.

Notches can be classified into many different categories, depending on their shapes, location within a structure, material recurrence or material manufacturing technology. They all have one common characteristic – they cause a local increase of stress in the structure under load, and thus influence its durability and strength.

On the basis of observation and experiments, scientists have been trying for so long to define some critical conditions, at which material is damaged. Reference can be made to e.g. ideas by Galileo, Tresca, Beltrami, Coulomb, Mohr, Mises or Huber. They adopted some hypotheses, defining material strength, that until now are the basis for engineering calculations. Assuming homogeneity and continuity of a medium, of which a structural element has been made, they formulated limit values for a function, the exceeding of which resulted in

material damage. These hypotheses did not take into account the significant influence of stress and strain field gradients on the strength. Theoretical development in solid state mechanics, and in theory of elasticity, in particular, has allowed for obtaining many analytical solutions describing local stress fields in the surrounding of both soft concentrators (e.g. in Kirsch's solution [8]), and sharp concentrators, generating singular stress fields (Sneddon's [31], and Williams' solutions [38]). Knowledge of new mathematical solutions has enabled formulation of consequent strength criteria including the influence of the presence of stress concentrators in homogeneous structural materials (e.g. Griffith [6], Sih [29], McClintock [16] and others).

Over the recent years, there has been a noticeable development of composite materials with pre-designed mechanical properties. As a rule, these are anisotropic materials or composites of a complex periodic structure.

Typical stress concentrator, present in layered composites, is a crack [30] or sharp notch located in the plane of bonding particular layers which form a composite [3, 5, 26]. Such concentrators are frequently present also in structural elements made by bonding two different materials with adhesive (such element can be considered a specific composite material). It is therefore necessary to define strength and resistance to cracking of composites (including mechanical properties of a bonding layer), where structural notches generate large stress gradients. A solution for this problem is an adequately formulated strength criterion. This criterion should include accurately determined equation with defined material constants, on basis of which it is possible to predict the moment of cracking process initiation. Predicting durability of elements with structural notches has not been the field of study taken by many scientists. In paper [12]

---

strength of two-phase elements with the structural notch was analysed experimentally. Material components were adhesive bonded. The authors performed three-point bending tests and determined values of crack initiation forces. A possibility of applying Leguillon's criterion for this type of elements (adhesive bonded uniform component with notch) was verified positively in paper [36].

As regards criteria for bi-material structures there are no available results published in the literature. The criterion that is frequently applied to homogeneous materials is the MClintock criterion. Thus, the main objective of this paper is to experimentally verify the possibility of applying this criterion (with appropriate modifications) for bi-material structures, where sharp structural notches generate singular stress fields. An idea for the criterion is described below.

Notations and Nomenclatures

a - Notch height

b - Gradient of combined stress

E - Young's modulus

f_{ik}^{I}, f_{ik}^{II} -Influence coefficient for stress

F - Load force at which stress intensity factors were calculated

F_k - Predicted critical force

g - Specimen thickness

h - Specimen height

H_o, H_1, H_2 - Influence coefficient for the characteristic equation

i - Material index (=1,2)

j - Generalised stress intensity factors/ Combined stresses index (=I,II)

K_E - Equivalent stress intensity factor

K_{Ec} - Critical value of the equivalent stress intensity factor

K_I, K_{II} -Generalised stress intensity factors

K_{Ic} - Fracture toughness

L - Spacing between supports set in the three-point bending test

Lc -Total specimen length

n - Nodes index

r, φ -Polar coordinates

u_r, u_φ - Displacements in polar coordinates

u_y - Vertical displacement applied as load condition in FEM simulations

α - Angle between the edge of material 1 and interface

β - Notch-tip angle

γ - Angle between the edge of material 2 and interface

Γ - Shear modulus' ratio

δ - Imaginary part of eigenvalue λ

λ - Eigenvalue

λ_r - Real part of eigenvalue λ

μ - Shear modulus

ν - Poisson's ratio

$\sigma_\varphi, \sigma_r, \tau_{r\varphi}$ -Stresses in polar coordinates

φ_0 - Cracking propagation angle

ψ -Mode mixity ratio

2. Fracture Criterion

With criterion proposed in paper [16] it is assumed that cracking will follow, if normal strain ε_φ in some small distance from the crack tip ρ_c reaches a critical value which can be noted as follows:

$$\varepsilon_\varphi(\rho_c) = \varepsilon_c \qquad (1)$$

However, such stress form of this criterion, where the strain was replaced by an adequate component of normal stresses, had broader application.

In the approach as proposed in paper [23] it was assumed that propagation of cracking will follow only if circumferential stresses σ_φ at some finite distance $r = \rho_c$ reach critical value σ_c (2). Use of the condition formulated in such way, for elements with notches present in homogeneous materials, has been positively verified in many papers, e.g. [27]:

$$\max_{\varphi} \sigma_\varphi(\rho_c) = \sigma_c \qquad (2)$$

Cracking propagation angle φ_0 is determined by maximizing σ_φ in relation to angle φ. For the elements with the notch located on adhesive bonding of uniform or bi-material structure, the cracking initially propagates along the interface. Thus, it can be predicted that $\varphi_0 = 0$ (Fig. 1) and the condition (2) will be written as:

$$\sigma_\varphi(\rho_c, 0) = \sigma_c \qquad (3)$$
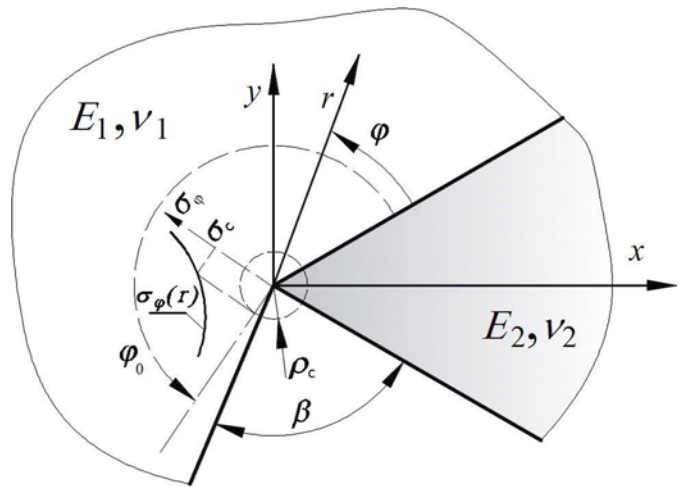
Fig. 1. Graphic interpretation McClintock criterion.

The parameter ρ_c, is considered as material constant and can be determined from experiment. For example, in condition (3), by taking advantage of dependence on circumferential stresses at crack tip and Griffith – Irwin criterion, the following is obtained:

$$\frac{K_{Ic}}{\sqrt{2\pi\rho_c}} = \sigma_c \qquad (4)$$

and thus this allows for calculating the characteristic constant:

$$\rho_c = \frac{1}{2\pi}\left(\frac{K_{Ic}}{\sigma_c}\right)^2, \qquad (5)$$

where K_{Ic} - fracture toughness, σ_c - tensile strength.

One advantage of the proposed method which is based on the so-called Theory of Critical Distances (TDC), is that in most cases in order to predict the fracture process it is not required to know the asymptotics description of stress fields - numerical solutions are used in the predicting process.

In the case when the fracture process occurs in a plane in which complex state of stresses is present, the use of numerical solutions may result in an erroneous prediction [13]. Most frequently in such situation, on the basis of analytical description of local stress fields, a global fracture criterion (using local parameter ρ_c) is formulated and it is based on an equivalent stress intensity factor [1, 13, 27] or minimum strain-energy density [9].

In this paper, on the basis of McClintock criterion, two concepts of prediction of fracture process initiation are proposed. First of them is based on an equivalent stress intensity factor, and the other on a dependence of condition (2) of critical stresses on proportions of shear and normal stresses occurring in the cracking plane. Detailed description of the concept is presented in section 6.

As it can be seen, when using the McClintock criterion for elements simultaneously loaded with shear and normal loads, it is required to know the distribution of stress fields occurring in the immediate vicinity to a singular point. Therefore, in the next section herein, forms of functions describing such stress fields and methodology of their determining will be discussed.

3. Analytical relations describing stress fields present in structural notch-tip area

A solution of the case of bi-material with the structural notch located on the interface (Fig. 2) was obtained using the approach applied by the authors of paper [21] for sharp corner in a uniform material.
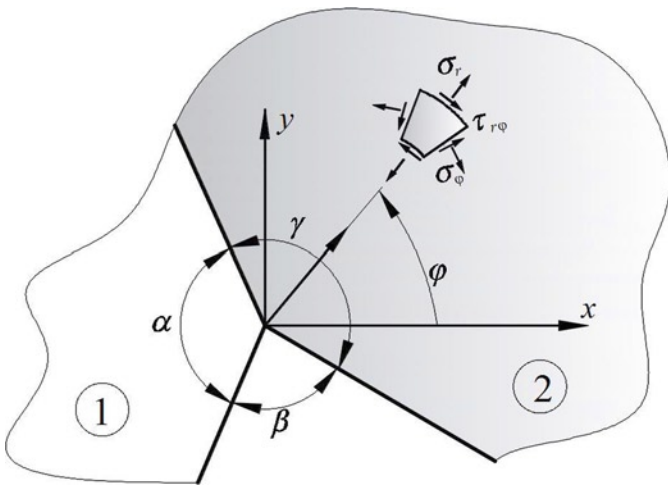
Fig. 2. Bi-material with structural notch located on interface

In the used method, the detailed description of which can be found in paper [19], by applying Airy's stress function it is possible to obtain general asymptotic solutions describing individual components of stress fields and displacements. For the analyzed bi-material structure the general asymptotic solutions are given by [18]:

$$u_{ri} = r^\lambda \left(A_i \cos\left((1+\lambda)\varphi\right) + B_i \sin\left((1+\lambda)\varphi\right) + C_i \cos\left((1-\lambda)\varphi\right) + D_i \sin\left((1-\lambda)\varphi\right) \right)$$

$$u_{\varphi i} = r^\lambda \left(-A_i \sin\left((1+\lambda)\varphi\right) + B_i \cos\left((1+\lambda)\varphi\right) - C_i \frac{\kappa+\lambda}{\kappa-\lambda} \sin\left((1-\lambda)\varphi\right) + D_i \frac{\kappa+\lambda}{\kappa-\lambda} \cos\left((1-\lambda)\varphi\right) \right)$$

$$\sigma_{ri} = r^{\lambda-1}\mu\left(A_i 2\lambda \cos\left((1+\lambda)\varphi\right) + B_i 2\lambda \sin\left((1+\lambda)\varphi\right) + C_i (3-\lambda)\frac{2\lambda}{\kappa-\lambda}\cos\left((1-\lambda)\varphi\right) + D_i (3-\lambda)\frac{2\lambda}{\kappa-\lambda}\sin\left((1-\lambda)\varphi\right) \right)$$

$$\sigma_{\phi i} = r^{\lambda-1}\mu\left(-A_i 2\lambda \cos\left((1+\lambda)\varphi\right) - B_i 2\lambda \sin\left((1+\lambda)\varphi\right) + C_i (1+\lambda)\frac{2\lambda}{\kappa-\lambda}\cos\left((1-\lambda)\varphi\right) + D_i (1+\lambda)\frac{2\lambda}{\kappa-\lambda}\sin\left((1-\lambda)\varphi\right) \right)$$

$$\tau_{r\phi i} = r^{\lambda-1}\mu\left(-A_i 2\lambda \sin\left((1+\lambda)\varphi\right) + B_i 2\lambda \cos\left((1+\lambda)\varphi\right) + C_i (1-\lambda)\frac{2\lambda}{\kappa-\lambda}\sin\left((1-\lambda)\varphi\right) - D_i (1-\lambda)\frac{2\lambda}{\kappa-\lambda}\cos\left((1-\lambda)\varphi\right) \right).$$

$$(6)$$

where: $\mu_i = \dfrac{E_i}{2(1+\nu_i)}$ -shear modulus $\kappa_i = (3-\nu_i)/(1+\nu_i)$ - a plane stress, $\kappa_i = (3-4\nu_i)$ - a plane strain, ν_i -Poisson's ratio, i=1.2.

Particular solution is obtained by determining exponent λ and constants A_i, B_i, C_i, D_i. Constants are determined on basis of the following boundary conditions [18]:

1. of the left side surface of V-notch, for $\varphi = \alpha$;
$$\sigma_{\varphi 1} = \tau_{r\varphi 1} = 0$$

2. of the left side surface of V-notch, for $\varphi = -\gamma$;
$$\sigma_{\varphi 2} = \tau_{r\varphi 2} = 0$$

3. along the interface, for $\varphi = 0$;
$$u_{r1} = u_{r2}; u_{\varphi 1} = u_{\varphi 2};\ \sigma_{\varphi 1} = \sigma_{\varphi 2}; \tau_{r\varphi 1} = \tau_{r\varphi 2},$$

Moreover on basis of condition of zeroing matrix determinant of matrix boundary conditions the characteristic equation (7) can be determined, the individual roots of which determine the value of exponent λ in obtained asymptotic solutions (6). The characteristic equation takes the form [18]:

$$H_0 + \Gamma H_1 + \Gamma^2 H_2 = 0 \qquad (7)$$

where:

$$H_o = \left(1-2\lambda^2 + 2\lambda^2\cos[2\alpha]\right)\left(1-\lambda^2+\lambda^2\cos[2\gamma]-\cos[2\gamma\lambda]\right) - \kappa_1\left\{\cos\left[2(-\alpha+\gamma)\lambda\right] + \cos\left[2(\alpha+\gamma)\lambda\right] + \cos[2\alpha\lambda]\left(-2+4\lambda^2\sin[\gamma]^2\right) + 2\left(\lambda^2\sin[\gamma]^2 - \sin[\gamma\lambda]^2\right)\kappa_1\right\}$$

$$H_1 = 5\lambda^2 + \cos[2\alpha\lambda] + \cos[2\gamma\lambda] - 2\cos\left[(-\alpha+\gamma)\lambda\right]^2 - \lambda^2\left(3\cos[2\alpha] - \cos[2(\alpha-\gamma)] + 3\cos[2\gamma] + 4\cos[2\gamma\lambda]\sin[\alpha]^2 + 4\left(\cos[2\alpha\lambda]+4\lambda^2\sin[\alpha]^2\right)\sin[\gamma]^2\right) + \kappa_2\left(\cos\left[2(\alpha+\gamma)\lambda\right] - \cos[2\alpha\lambda] + 2\sin[\gamma\lambda]^2 - \lambda^2\left(1+\left(\cos[2\alpha]+4\cos[2\gamma\lambda]\sin[\alpha]^2 - 2\sin[\alpha]\sin[\alpha-2\gamma]\right)\right)\right) + \kappa_1\left\{\cos\left[2(\alpha+\gamma)\lambda\right]+4\lambda^2\cos[\alpha]\sin[\alpha-\gamma]\sin[\gamma]+\cos[2\alpha\lambda]\left(-1+4\lambda^2\sin[\gamma]^2\right)+2\sin[\gamma\lambda]^2 + \left(\cos[2\alpha\lambda]+\cos[2\gamma\lambda]-2\cos\left[(-\alpha+\gamma)\lambda\right]^2+4\lambda^2\cos[\alpha-\gamma]\sin[\alpha]\sin[\gamma]\right)\kappa_2\right\},$$

$$H_2 = \left(1-2\lambda^2+2\lambda^2\cos[2\gamma]\right)\left(1-\lambda^2+\lambda^2\cos[2\alpha]-\cos[2\alpha\lambda]\right) - \kappa_2\left\{\cos\left[2(-\alpha+\gamma)\lambda\right]+\cos\left[2(\alpha+\gamma)\lambda\right]+\cos[2\gamma\lambda]\left(-2+4\lambda^2\sin[\alpha]^2\right)+2\left(\lambda^2\sin[\alpha]^2-\sin[\alpha\lambda]^2\right)\kappa_2\right\},$$

$$\Gamma = \frac{\mu_1}{\mu_2}.$$

On the basis of the characteristic equation (7) it can be inferred that eigenvalue λ depends on material constants and notch-tip angle. The roots of equation (7) cannot be determined analytically. They were calculated numerically. To this end, a special program was created in the Mathematica software.

Fig. 3 graphically illustrates solution of equation (7), where thick line was used to mark real eigenvalues λ ($\lambda = \lambda_r$, Im[λ]=0), while thin line – to mark real parts of complex eigenvalues λ (λ_r=Re[λ],

Im[λ]=δ), and dotted line – to mark imaginary parts of complex eigen-values λ (δ = Im[λ]).
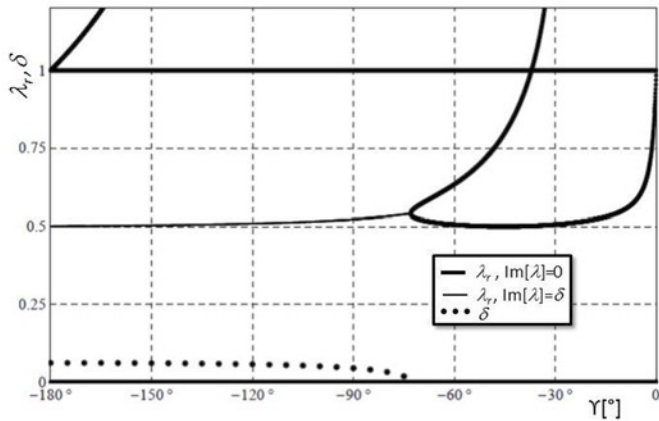
Fig. 3. Solution of the characteristic equation (7) for Γ = 0.033, α=180˚, ν₁=0.37, ν₂=0.35, (plane strain)

The solution obtained implies that depending on material constants and notch geometry, there can be one or more singularities with a real or complex exponent λ. What is more, it is worth noting that for the notch problem located in the multi-material, the characteristic equations cannot be obtained independently for mode I and mode II [3, 5]

Since stresses can be described with complex exponent λ, generalised stress intensity factors were defined alike the authors of paper [32] (for the interfacial crack):

$$\left(\sigma_\varphi + i\tau_{r\varphi}\right)_{\varphi=0} = \frac{K_I + iK_{II}}{\sqrt{2\pi}r^{1-\lambda_r}}\left(\frac{r}{2a}\right)^{i\delta}\cosh\left[\pi\delta\right], \qquad (8)$$

where dimension *a* can be considered as e.g. notch height.

Using an equation (6), boundary conditions and the adopted generalized stress intensity factors definition (8), an analytical description of the stress fields occurring in the notch tip area can be obtained [18]:

$$\sigma_{ik} = \frac{\cosh\left[\pi\delta\right]\sqrt{K_I^2 + K_{II}^2}}{\sqrt{2\pi}r^{1-\lambda_r}}\left(\sin\left[\arctan\left[\frac{K_{II}}{K_I}\right] + \delta\log\left[\frac{r}{2a}\right]\right]\mathrm{Re}\left[f_{ik}^I\right] + \cos\left[\frac{K_{II}}{K_I} + \delta\log\left[\frac{r}{2a}\right]\right]\mathrm{Re}\left[f_{ik}^{II}\right]\right), \qquad (9)$$

where:

$$f_{rr}^I = M^{-1}\left(\begin{matrix}(\lambda-1)\cos\left[(1+\lambda)\varphi\right]\left(\lambda\sin\left[2\epsilon\right]-\sin\left[2\epsilon\lambda\right]\right)-(1+\lambda)\left(\lambda-\lambda\cos\left[2\epsilon\right]+\cos\left[2\epsilon\lambda\right]-1\right)\sin\left[(1+\lambda)\varphi\right] \\ +(\lambda-3)\left(\lambda\sin\left[2\epsilon+(\lambda-1)\varphi\right]+(1+\lambda)\sin\left[\varphi-\lambda\varphi\right]-\sin\left[2\epsilon+\varphi-\lambda\varphi\right]\right)\end{matrix}\right),$$

$$f_{rr}^{II} = -M^{-1}\left(\begin{matrix}(1-\lambda)\left(\lambda\cos\left[2\epsilon\right]+\cos\left[2\epsilon\lambda\right]-1-\lambda\right)\cos\left[(1+\lambda)\varphi\right]+ \\ (\lambda-3)\left(-\lambda\cos\left[2\epsilon+(\lambda-1)\varphi\right]+(\lambda-1)\cos\left[\varphi-\lambda\varphi\right]+\cos\left[2\epsilon\lambda+\varphi-\lambda\varphi\right]\right)- \\ +(\lambda-1)\left(\lambda\sin\left[2\epsilon\right]+\sin\left[2\epsilon\lambda\right]\right)\sin\left[(1+\lambda)\varphi\right]\end{matrix}\right),$$

$$f_{\varphi\varphi}^I = M^{-1}(1+\lambda)\left(\begin{matrix}(1-\lambda)\sin\left[(1+\lambda)\varphi\right]+\lambda\sin\left[2\epsilon+(\lambda-1)\varphi\right]+ \\ (1+\lambda)\sin\left[\varphi-\lambda\varphi\right]-\sin\left[2\epsilon\lambda+\varphi-\lambda\varphi\right]-\lambda\sin\left[2\epsilon-(1+\lambda)\varphi\right]+\sin\left[2\epsilon\lambda-(1+\lambda)\varphi\right]\end{matrix}\right),$$

$$f_{\varphi\varphi}^{II} = -M^{-1}\left(\begin{matrix}(\lambda-1)\left(-1-\lambda+\lambda\cos\left[2\epsilon\right]+\cos\left[2\epsilon\lambda\right]\right)\cos\left[(1+\lambda)\varphi\right]+(\lambda-1)\left(\lambda\sin\left[2\epsilon\right]+\sin\left[2\epsilon\lambda\right]\right)\sin\left[(1+\lambda)\varphi\right] \\ +(1+\lambda)\left(\lambda\cos\left[2\epsilon+(\lambda-1)\varphi\right]-\lambda\cos\left[\varphi-\lambda\varphi\right]+2\sin\left[\epsilon\lambda\right]\sin\left[\epsilon+\varphi-\lambda\varphi\right]\right)\end{matrix}\right),$$

$$f_{r\varphi}^I = M^{-1}\left(\begin{matrix}(1+\lambda)\left(1-\lambda+\lambda\cos\left[2\epsilon\right]-\cos\left[2\epsilon\lambda\right]\right)\cos\left[(1+\lambda)\varphi\right]+ \\ (\lambda-1)\left(\lambda\cos\left[2\epsilon+(\lambda-1)\varphi\right]-(1+\lambda)\cos\left[\varphi-\lambda\varphi\right]+\cos\left[2\epsilon\lambda+\varphi-\lambda\varphi\right]\right)+ \\ +(1+\lambda)\left(\lambda\sin\left[2\epsilon\right]-\sin\left[2\epsilon\lambda\right]\right)\sin\left[(1+\lambda)\varphi\right]\end{matrix}\right),$$

$$f_{r\varphi}^{II} = M^{-1}(\lambda-1)\left(\begin{matrix}(1+\lambda)\sin\left[(1+\lambda)\varphi\right]-\lambda\sin\left[2\epsilon+(\lambda-1)\varphi\right] \\ -(\lambda-1)\sin\left[\varphi-\lambda\varphi\right]-\sin\left[2\epsilon\lambda+\varphi-\lambda\varphi\right]+\lambda\sin\left[2\epsilon-(1+\lambda)\varphi\right]+\sin\left[2\epsilon\lambda-(1+\lambda)\varphi\right]\end{matrix}\right),$$

$$M = 2\left(\lambda^2-\lambda^2\cos\left[2\epsilon\right]+\cos\left[2\epsilon\lambda\right]-1\right), \epsilon = \alpha \text{ -for the material 1 and } \epsilon = -\gamma$$

for the material 2.

Below a particular form of stress fields for angle φ=0, i.e. along the interface line is presented [18]:

$$\sigma_{\varphi 1,2_{\varphi=0}} = \frac{1}{\sqrt{2\pi}}\sqrt{K_I^2 + K_{II}^2}\, r^{\lambda_r-1}\cos\left[\arctan\left[\frac{K_{II}}{K_I}\right]+\delta\ln\left[\frac{r}{2a}\right]\right]\cosh\left[\pi\delta\right],$$

$$\tau_{r\varphi 1,2_{\varphi=0}} = \frac{1}{\sqrt{2\pi}}\sqrt{K_I^2 + K_{II}^2}\, r^{\lambda_r-1}\sin\left[\arctan\left[\frac{K_{II}}{K_I}\right]+\delta\ln\left[\frac{r}{2a}\right]\right]\cosh\left[\pi\delta\right].$$

$$(10)$$

When the exponent is a real value (δ = 0) dependence (10) will be simplified to the following form:

$$\sigma_{\varphi 1,2_{\varphi=0}} = \frac{1}{\sqrt{2\pi}}K_I\, r^{\lambda_r-1}, \tau_{r\varphi 1,2_{\varphi=0}} = \frac{1}{\sqrt{2\pi}}K_{II}\, r^{\lambda_r-1}. \quad (11)$$

For a quantitative description of stresses, it is necessary to determine values of K_j. They were determined based on comparing the obtained analytical solutions with stresses obtained from *FEM* solution. Due to the fact that the main purpose of the presented paper was experimental verification of possibilities of using the McClintock criterion, *FEM* models of specimens were prepared, the strength of which was tested by means of experiments in [11, 12].

4. Testing specimens and FEM model

Specimens were modelled in numerical simulations, the geometry and material properties of which were identical as in specimens used in experimental testing (prepared by authors of papers [11, 12]).
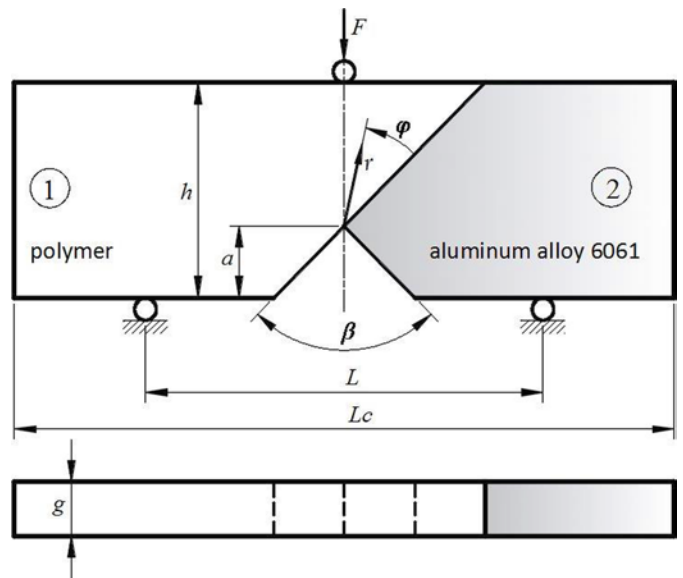
Fig. 4. Geometry and load of specimens with structural notch

Two types of specimens were analysed:
– component 1 made of PC (Polycarbonate) while component 2 of aluminum alloy 6061;

– component 1 made of PMMA (Poly(methyl methacrylate)) while component 2 of aluminum alloy 6061.

Components were bonded using Weld-on® 10 adhesive. The adhesive has been selected so that its stiffness properties were close to those of polymers. Therefore, it was possible to confirm the assumption that it is the bi-material that is modelled, not a three-layer composite. In this case, the adhesive interface could be treated as a layer without any thickness, but with different strength and fracture toughness than the polymers or the aluminum alloys separately. During the bonding process, achieving the minimum adhesive thickness was one of the goals. To obtain the minimum thickness of the adhesive, the specimens were joint under high pressure using a special holder. They were allowed to cure for a period of 24 hours to achieve the required bonding strengths. The thickness of the adhesive layer was not measured. Such information was not needed for the prediction of fracture toughness, assuming that the analyzed structure is the bi-material.

It is worth noting that using the selected adhesive in case where two different metal alloys are being combined, e.g. steel and aluminum alloy, ignoring the adhesive layer thickness and treating such a structure as a bi-material would be unacceptable. In that case, the approach based on the Traction-Separation criterion [25] can be used to predict the critical load. Namely, the adhesive layer should be modeled using special finite elements (cohesive elements). To define such elements it is necessary to know such parameters as maximum normal traction at the interface, normal separation across the interface where the maximum normal traction is attained and the limit value of separation. These parameters can be determined, knowing the thickness of the adhesive layer, based on experimental tests.

The carried out analyses were aimed at determining the applicability of the proposed fracture criterion for bi-material structures in a situation where a complex state of stress occurs on the interface, and the structural notch generates singular stress fields. Whereby the stress fields, depending on the geometrical and material features of the structure, can be described using real or complex λ exponents. Specimens with different notch-tip β angle were used in the study. β angles were selected in a way to obtain instances when stresses are described both in real and complex λ exponent. What's more, the variation of the notch-tip angles allowed for obtaining different proportions of tangential and normal stresses occurring in the plane of the connection. In all specimens, equal notch height a (measured from the lower surface of the sample), overall dimensions and the position of the support and loading points in the three-point bending test were assumed. This was to ensure the same boundary conditions (fixing and loading) for all examined specimens. Overall dimensions were chosen arbitrarily considering the capabilities of both the research stand and the device used for specimen preparation.

Specimen dimensions were as follows: total length Lc=254 mm, a spacing between supports L=90 mm, notch height a=19.1 mm, sample height h=50.8 mm, thickness g=5.4 mm, respectively. As regards the notch-tip angle $β$, three cases were considered: $β$= 30°, $β$= 90° and $β$= 120°. The specimens used in the tests are presented in Table 1. Material specification for individual components is given in Table 2.

Table 2. Mechanical properties of individual components of specimens [12]

	Young's modulus E [GPa]	Poisson's ratio $ν$
aluminum alloy 6061	70	0.35
PC	2.38	0.37
PMMA	3.79	0.37

Table 1. Tested bi-material structure

No	Tested bi-material structure	Notch-tip angle $β[°]$
1	PC/ aluminum alloy 6061	30
2	PC/ aluminum alloy 6061	90
3	PC/ aluminum alloy 6061	120
4	PMMA/ aluminum alloy 6061	30
5	PMMA/ aluminum alloy 6061	90
6	PMMA/ aluminum alloy 6061	120

Tested specimens (Fig. 4, Tab. 1) were modelled with *FEM*, using ANSYS application. Fig. 5 shows, for a given specimen, division to finite elements and boundary conditions.
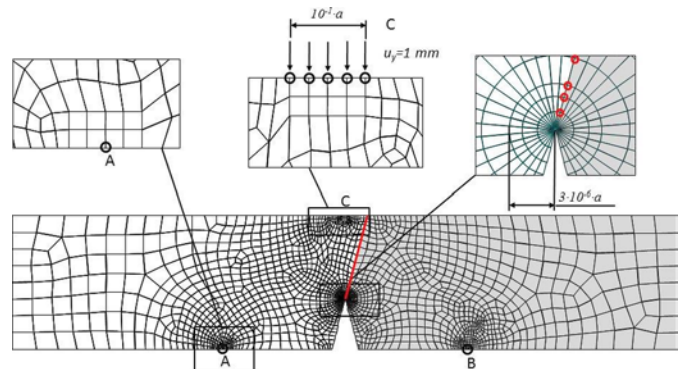
Fig. 5. Division to finite elements and conditions of mounting and loading of the specimen with notch with tip angle β= 300, the red colour was used to mark nodes from which the stresses were read for stress intensity factors calculation

Plane specimens were described with quadrangle, eight-node finite elements with increased refinement (according to the arithmetic series) in the tip area, with triangular special elements [35] surrounding singular point (Fig. 5). The total length of the lateral edges of the last three elements depended on the notch height a and were assumed to be $3 \cdot 10^{-6}\ a$ for all specimens. Due to the high density of the finite element mesh in the notch tip area, the prepared models contained approximately 10000 finite elements. As already mentioned before, the specimens can be treated as a bi-material structure. Therefore, the adhesive layer was not included in the prepared numerical models. As for the connection conditions of individual components, the nodes laying on the interface were shared between both materials. There was not allowed for slip between components on the interface.

Due to the fact that it is difficult to determine real frictional conditions of the contact between supports and material of the specimen, which are present during the three-point bending test, certain simplifications should be adopted. Thus, two methods of mounting were tested:

I   sliding supports (disabled possibility of moving vertically in nodes located in support points A and B);

II   non-sliding supports (disabled possibility of moving vertically and horizontally in nodes located in support points A and B).

As regards the load conditions, the specimens were loaded with a constant vertical displacement u_y = 1mm, applied at selected nodes (point C). Loading force F was determined on the basis of stresses in the nodes to which the displacement u_y was applied.

Numerical calculations were carried out for plane stress and plane strain cases.

As already mentioned before, in the FEM models, the adhesive, as a separate material layer, was not included. Despite this, it was possible to include the interface's strength properties in the used fracture criterion. On the basis of numerical simulations, stress intensity factors were determined. They were used to calculate the value of the predicted failure function (described further in the paper), which were then compared with the critical values. The interface's strength properties in the tested specimens was taken into account in that the critical values of the failure function and the ρ_c parameter were determined based on the bonding tensile strength and bonding fracture toughness (Tab. 3). Both of parameters were determined experimentally for the bi-materials made of PMMA and aluminum alloy as well as PC and aluminum alloy.

5. Description of method applied to determine generalised stress intensity factors

To determine values of generalised stress intensity factors K_j extrapolation method was applied. This method, unlike e.g. energy methods [37], or methods based on the application of special finite elements [4], is less complex. The disadvantage of this method, though, is a necessity to use a high density of mesh of division to finite elements in the tip area of stress concentrator. Additionally, accuracy of the results is influenced by the selection of area, where the numerical solution is compared with the analytical solution. This inconvenience can be eliminated by using terms of higher order [17, 24, 33] in the analytical description or determining an adequate criterion for the selection of nodes, for which values of stresses obtained from FEM modelling are compared with the known analytical solution. Such criterion was specified in papers [20] (for the case of interfacial crack) and [18] (for the problem of structural notch). As is well known, if the stress chart of the type $\sigma = Ar^{-b}$ in logarithmic system is linear, the line gradient equals -b.
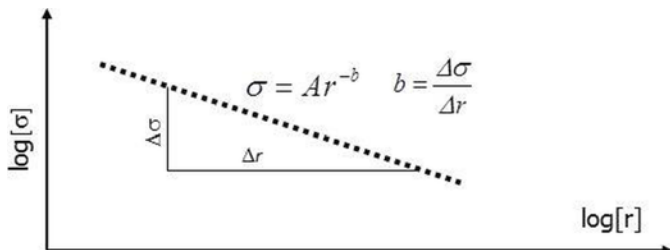
Fig. 6. Graphical interpretation of singular stress fields with theoretical gradient b [18]

Thus, when determining stress intensity factors, numerical and analytical solutions are compared only for nodes with the gradient of b.

For the case of the structural notch, stress components are always simultaneously dependent on K_I and K_{II}, and therefore, in order to use the above criterion, it is necessary to determine the so-called "combined stresses" [18]:

$$\sigma_I(r,0) = Sech[\pi\delta]\left(\sigma\cos\left[\delta\ln\left[\frac{r}{2a}\right]\right]+\tau\sin\left[\delta\ln\left[\frac{r}{2a}\right]\right]\right)=\frac{K_I}{\sqrt{2\pi}r^{1-\lambda_r}},$$

(12)

$$\sigma_{II}(r,0) = \left(\tau\cos\left[\delta\log\left[\frac{r}{2a}\right]\right]-\sigma\sin\left[\delta\log\left[\frac{r}{2a}\right]\right]\right)Sech[\pi\delta]=\frac{K_{II}}{\sqrt{2\pi}r^{1-\lambda_r}},$$

(13)

where - σ, τ are circumferential and shear stresses, respectively, obtained from *FEM* modelling (obtained from nodes located on the interface).

According to the adopted criterion when determining the sought generalised stress intensity factors, pairs of nodes with the gradient of $b=(\lambda_r-1)\pm 0.01$ were taken into account.

The "combined stresses" $\sigma_j(r,0)$ in the distance of r_n and r_{n+1} from the notch tip can be noted as follows:

$$\sigma_j(r_n,0)=\frac{K_j}{\sqrt{2\pi}r^{1-\lambda_r}}(1+cr_n),\sigma_j(r_{n+1},0)=\frac{K_j}{\sqrt{2\pi}r^{1-\lambda_r}}(1+cr_{n+1}).$$

(14)

Using equations (12) – (14) after simple mathematical transformations, formulas (15) are obtained: (enabling to determine factors K_j at some distance from the notch tip):

$$K_I=\frac{\sqrt{2\pi}\,(r_nr_{n+1})^{1-\lambda_r}}{r_n-r_{n+1}}sech[\pi\delta]\left\{r_n^{\lambda_r}\left(\sigma_{(r_{n+1})}\cos\left[\delta\ln\left[\frac{r_{n+1}}{2a}\right]\right]+\tau_{(r_{n+1})}\sin\left[\delta\ln\left[\frac{r_{n+1}}{2a}\right]\right]\right)-\right.$$
$$\left. r_{n+1}^{\lambda_r}\left(\sigma_{(r_n)}\cos\left[\delta\ln\left[\frac{r_n}{2a}\right]\right]+\tau_{(r_n)}\sin\left[\delta\ln\left[\frac{r_n}{2a}\right]\right]\right)\right\}$$
$$K_{II}=\frac{\sqrt{2\pi}\,(r_nr_{n+1})^{1-\lambda_r}}{r_n-r_{n+1}}sech[\pi\delta]\left\{r_n^{\lambda_r}\left(\tau_{(r_{n+1})}\cos\left[\delta\ln\left[\frac{r_{n+1}}{2a}\right]\right]-\sigma_{(r_{n+1})}\sin\left[\delta\ln\left[\frac{r_{n+1}}{2a}\right]\right]\right)-\right.$$
$$\left. r_{n+1}^{\lambda_r}\left(\tau_{(r_n)}\cos\left[\delta\ln\left[\frac{r_n}{2a}\right]\right]-\sigma_{(r_n)}\sin\left[\delta\ln\left[\frac{r_n}{2a}\right]\right]\right)\right\}$$

(15)

Calculated stress intensity factor, for selected nodes (with the gradient of $b=(\lambda_r-1)\pm 0.01$), is approximated with a straight line and this way generalised stress intensity factors K_j are determined.

It is worth noting that if exponent λ is a real number ($\delta=0$), the dependence (15) is simplified to the form as given in paper [14]:

$$K_I=\frac{\sqrt{2\pi}\,(r_nr_{n+1})^{1-\lambda_r}\left(r_{n+1}^{\lambda_r}\sigma_{(r_n)}-r_n^{\lambda_r}\sigma_{(r_{n+1})}\right)}{r_{n+1}-r_n}.$$

(16)

6. Test results and discussion

As it was already discussed, in order to verify the McClintock stress criterion, it is necessary to know the qualitative and quantitative description of stress fields which occurred in the cracking plane, critical parameters and experimental data (damage loads). Damage loads were taken from paper [11, 12]. Since after the cracking process was initiated, the crack propagated along the interface, in the tested criterion critical parameters characterising properties of adhesive layer / interface [10] were used, for which critical distance σ_c was determined, according to formula (5). The methods of determining critical parameters for the adhesive layer are discussed in [7, 10, 22, 25].

In order to determine the quantitative description of mechanical fields, generalised stress intensity factors K_j were calculated. They were determined numerically with extrapolation method using data obtained from *FEM* modelling and analytical solutions. The extrapolation method, *FEM* modelling and analytical solution were presented and discussed in the previous sections herein.

Values of the calculated generalised stress intensity factors K_j, for all types of samples (Fig. 4), are given in Tables 4-5.

Exponents λ, obtained from equation (7), for material constants given in Table 2, are listed in Table 6.

Table 3. Strength properties of adhesive - Weld-on® 10 [10]

	Tensile strength σ_c [MPa]	Fracture toughness K_{Ic} [MPa m$^{0.5}$]	Critical distance ρ_c [mm]
PC/ aluminum alloy 6061	11.35	0.24	0.071
PMMA/ aluminum alloy 6061	12.85	0.28	0.075

Table 4. Values of generalised stress intensity factors Kj and applied force F PC /aluminum alloy 6061

	mounting conditions					
	sliding supports			non-sliding supports		
β [°]	K_I [Pa m$^{1-\lambda r}$]	K_{II} [Pa m$^{1-\lambda r}$]	F [N]	K_I [Pa m$^{1-\lambda r}$]	K_{II} [Pa m$^{1-\lambda r}$]	F [N]
30	6621327.4* 5654415.8**	16207.8* 565904.7**	4139.0* 3508.3**	2670172.3* 2337935.8**	334892.9* 576351.2**	5598.9* 4718.3**
90	6953117.8* 7929593.6**	-2675922.6* -1851771.4**	3532.6* 3004.2**	2654647.7* 3089615.1**	-1281221.0* -622169.7**	5071.6* 4276.7**
120	3224964.6* 3206237.2**	-4631416.6* -6451442.2**	3345.1* 2853.9**	1156739.9* 1185145.1**	-1821056.5* -2538667.0**	5001.9* 4225.0**
*-plane strain, **-plane stress						

Table 5. Values of generalised stress intensity factors Kj and applied force F PMMA/aluminum alloy 6061

	mounting conditions					
	sliding supports			non-sliding supports		
β [°]	K_I [Pa m$^{1-\lambda r}$]	K_{II} [Pa m$^{1-\lambda r}$]	F [N]	K_I [Pa m$^{1-\lambda r}$]	K_{II} [Pa m$^{1-\lambda r}$]	F [N]
30	10590286.9* 9092521.1**	88797.8* 449519.4**	6510.0* 5522.1**	4304874.73* 3774299.6**	466048.7* 845462.9**	8818.2* 7435.5**
90	15655266.1* 13838295.9**	-8259321.6* -4731359.1**	5572.9* 4742.3**	6032440.86* 5427305.2**	-1915526.6* -578767.5**	8002.9* 6753.4**
120	4796910.9* 4040648.9**	-6494991.4* -6507052.4**	5279.8* 4507.1**	1798019.9* 1525983.9**	-2641592.9* -2594161.8**	7892.7* 6671.4**
*-plane strain, **-plane stress						

Table 6. Values of exponents λ

	type of specimen			
	PC/ aluminum alloy 6061		PMMA/ aluminum alloy 6061	
β [°]	λ_r	δ	λ_r	δ
30	0.5032* 0.5033**	0.0611* 0.0958**	0.5051* 0.5052**	0.0579* 0.0913**
90	0.5222* 0.5231**	0.0450* 0.0810**	0.5339* 0.5352**	0.0235* 0.0646**
120	0.5058* 0.5324**	0* 0**	0.5003* 0.5071**	0* 0**
*-plane strain, **-plane stress				

As already mentioned, if both shear and normal stresses are present in the cracking plane, in order to predict the cracking process the equivalent stress intensity factor K_E can be used. For the analysed case it is defined (on the basis of analytical description of local stress fields) using formula (17):

$$K_E = \cosh(\pi\delta)\sqrt{K_I{}^2 + K_{II}{}^2},\qquad(17)$$

Critical value of the factor K_{Ec} can be determined by solving the below system of equations (18):

$$\frac{\sigma_\varphi(\rho_c,0)}{\sigma_c} = 1, \left(\frac{\partial\sigma_\varphi}{\partial\varphi}\right)_{\varphi=0,r=\rho_c} = 0.\qquad(18)$$

After the system of equations (18) is solved - using formulas (5), (9) and (10) a dependence is obtained, allowing to determine the value of critical equivalent stress intensity factor (19):

$$K_{Ec} = (2\pi)^{\lambda_r - \frac{1}{2}} \left(\frac{K_{Ic}{}^2}{\sigma_c{}^2}\right)^{1-\lambda_r} \sigma_c.\qquad(19)$$

It is worth noting that for the tension element with a crack ($\lambda_r = 0.5$) or a notch, with tip angle equal to π ($\lambda_r = 1$), the dependence (19) is simplified accordingly to the following forms: $K_{Ec} = K_{Ic}; K_{Ec} = \sqrt{2\pi}\sigma_c$, which is consistent with the literature data.

Assuming that the fracture process will be initiated when:

$$K_E = K_{Ec},\qquad(20)$$

predicted critical force can be calculated from the following condition:

$$F_k = \frac{K_{Ec}F}{K_E},\qquad(21)$$

where F is a force at which K_E (17) were calculated.

As already mentioned it is difficult to model the actual frictional and contact conditions [2, 15] occurring in the support area with numerical modelling of three-point bending test. Therefore Figure 7 (for plane stress) and Table 7 (for plane strain) provide values for the predicted force F_k (21) determined by using two variants of specimen fixing in FEM models. It is obvious that the real critical force will take values from a range limited by forces estimated when using sliding supports and non-sliding supports in numerical models.

The values of critical forces determined using the formula (21) were compared with the experimental data, which is shown in Figure 7 and Table 6. The experimental crack initiation load is an average obtained from at least three experiments performed for each type of specimen.

On the basis of the obtained results it can be stated that distribution of the estimated critical forces is consistent with experimental data. Better convergence of results, both for plane stress and plane strain condition, was obtained by using non-sliding supports in the FEM model:

a)

b)
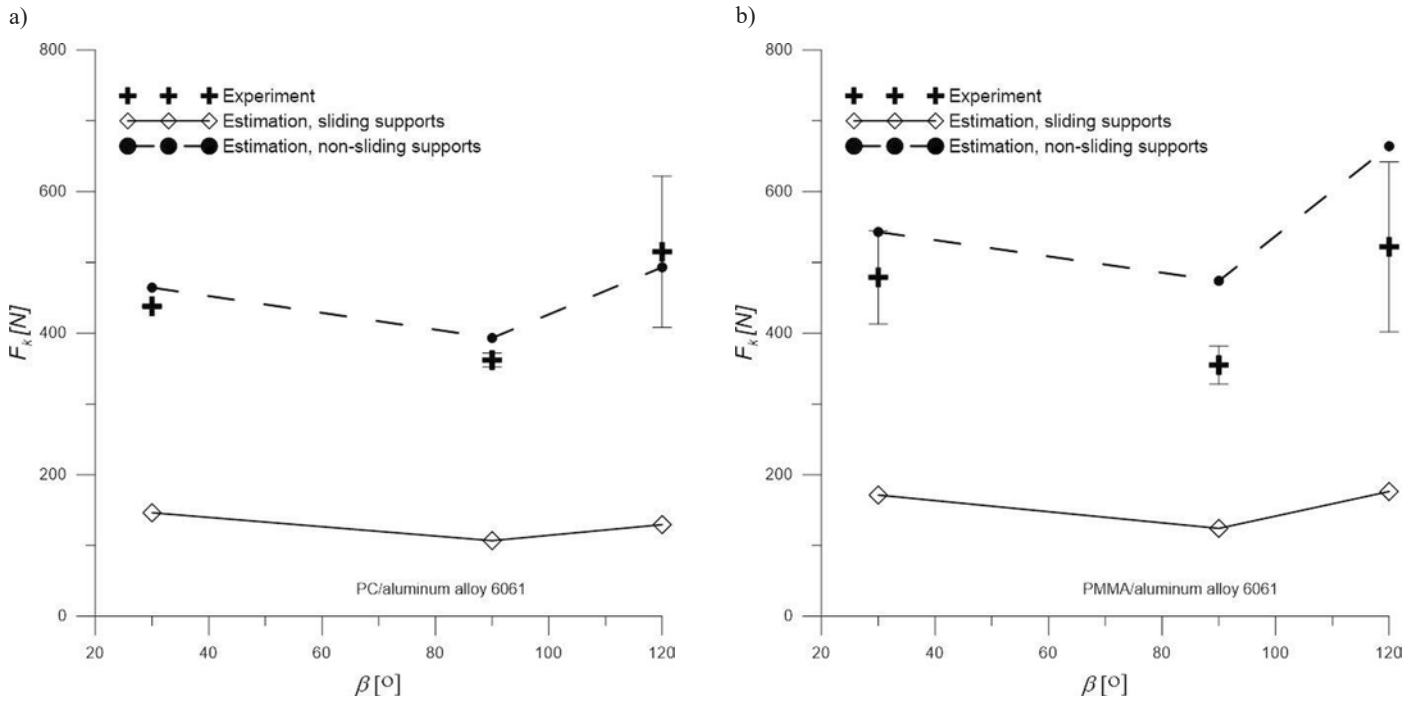
Fig. 7. Comparison of critical stress values, obtained from tested criterion with values obtained from experimental testing [12], bonded polycarbonate/ aluminum alloy 6061specimens, b) bonded PMMA/aluminum alloy 6061 specimens, plane stress

Table 7. Values of critical forces Fk (21) calculated for various types of specimens, plane strain

β [$^{\circ}$]	PC/ aluminum alloy 6061		PMMA/ aluminum alloy 6061	
	experiment [12]	estimation (21)	experiment [12]	estimation (21)
30	438±1	151.9* 505.7**	479±66	177.7* 588.6**
90	362±10	139.2* 403.3**	355±27	121.3* 487.2**
120	515±107	150.3* 587.9**	522±120	183.6* 693.6**
*- sliding supports, **- non-sliding supports				

When determining critical forces in the analytical description first singular term was used only. Use of terms of a higher order was not necessary due to a fact that analytical (when using the first singular term only) and numerical solutions matched one another in an area larger than the critical distance ρ_c, which is shown in Figure 8.

It is worth noting that prediction of fracture toughness with use of the concept of equivalent stress intensity factor is quite complicated. Since it is necessary to determine exponents λ and generalized stress intensity factors K_j. For uniform materials it is not a major problem, as approximate formulas are available which allow for calculation of generalized stress intensity factors, and exponent λ depends only on tip angle of the notch and can be easily determined (exponent values λ can be found, e.g. in paper [28]). For a bi-material with a notch situated on the interface, both K_j and λ depend on geometrical and material features of the structure and should be determined individually for each analysed case. Due to the above inconveniences, the paper attempts to develop a procedure of predicting fracture toughness which might be more practical from the engineering point of view.

Authors of many papers, e.g. [30] indicate that critical value of energy release factor depends on the ratio of shear and normal stresses which are present in the cracking plane. Therefore, critical stresses
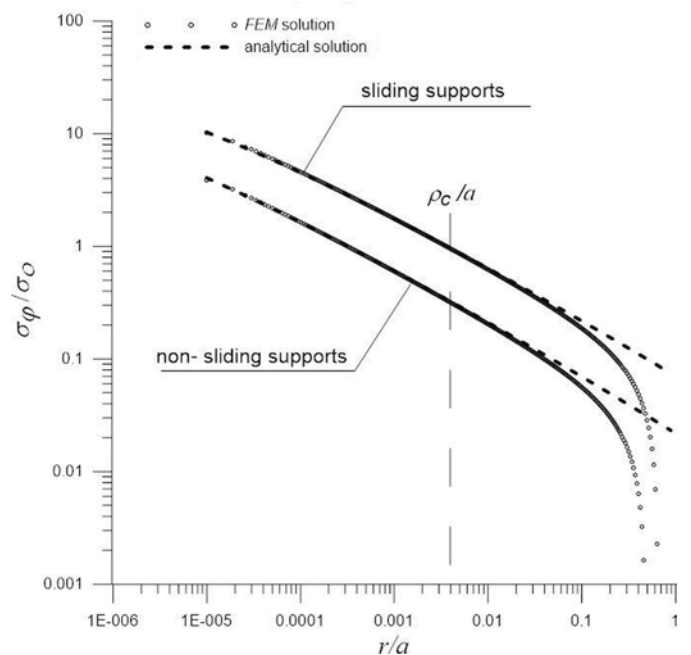
Fig. 8. The normalized circumferential stress versus r/a for PC/aluminum alloy 6061 specimen with notch-tip angle $\beta= 300$, $\sigma_0 = 3FL / \left(2gh^2\right)$, plane stress

also must be dependent on such factor. Accordingly, condition (3) can be written as follows (22):

$$\sigma_\varphi(\rho_c, 0) = \sigma_c(\psi) \qquad (22)$$

Taking into account inter-relationships between cracking mechanics parameters, the following form of function depending on critical stress to mode mixity ratio ψ was proposed:

$$\sigma_c\left(\psi\right) = \sigma_c \, / \sqrt{1+\psi^2}, \qquad (23)$$

where: $\psi = \dfrac{\tau_{r\varphi}\left(\rho_c, 0\right)}{\sigma_\varphi\left(\rho_c, 0\right)}$.

It is worth noting that the proposed modification of a criterion of cracking (23) is concurrent with a concept provided in paper [34]. Author of paper [34] suggests the use of an additional factor including impact of quantitative portion of shear and normal stresses in the process of prediction of crack initiation. This factor is not constant and depends on geometry of the object and load conditions.

By using criterion (23) critical force value can be estimated on the basis of dependence (24):

$$F_k = \frac{\sigma_c\left(\psi\right) F}{\sigma_\varphi\left(\rho_c, 0\right)}. \qquad (24)$$

Critical force F_k (24) can be determined in two ways:
– using analytical (qualitative description (9, 10)) and numerical (quantitative description (15)) solutions;
– using only numerical solution (stresses obtained, e.g. using FEM).

Of course the latter, from practical point of view, is less complicated and recommended for use in engineering calculations.

However in this paper the former is used. The reason for that was the necessity to check to what extent solutions obtained from formulas (21) and (24) match each other. Because critical forces (21) were estimated using analytical and numerical solutions, the same approach should be used in formula (24). Thus using analytical and numerical solutions, critical forces F_k (24) for all analysed specimens were determined. The obtained results were exactly the same as results obtained on the basis of formula (21) and therefore there was no need to include them in the paper.

7. Summary and conclusions

This paper dealt with the analysis of interface crack initiation at sharp notches along adhesive bonding in bonded bi-material structure. The possibility of using McClintock criterion was analysed to predict the loads at the crack initiation for such type of construction elements. In order to use this criterion, usually, it is necessary to know the qualitative and quantitative description of stress fields around concentrator's tip. Thus, the analytical description was obtained, and methodology of its obtaining was presented. Moreover, the method for determining generalised stress intensity factors was discussed, including qualitative nature of singularity of stresses fields, and for the selected cases, their values were determined.

The obtained analytical and numerical solutions allowed for formulation of the form of damage criterion and critical parameters.

Two forms of cracking criterion were developed, based on:
– equivalent stress intensity factor;
– modification of McClintock criterion involving dependence of critical stresses on proportion of shear and normal stresses occurring in the cracking plane.

The carried out analyses showed that from both forms of the cracking criterion the same results of prediction of critical forces are obtained. However from the practical point of view the second form of the cracking criterion is more favourable. This is due to the fact that in the prediction of cracking stresses determined by using, e.g. FEM can be used only with no need of determining stress intensity factors.

Values of critical loads resulting from the hypothesis were compared with values obtained from the experiment. Since actual frictional and contact conditions that are present in the specimen support area cannot be reflected with numerical modelling of three-point bending test, a range in which the predicted critical forces occur, was determined only. In the vast majority of analysed cases critical forces determined experimentally occurred in the range defined by means of the tested criterion. What is more, tendency of variability of the predicted forces was consistent with experimental data. This suggests that the analysed criterion can be used to predict initiation of the process of cracking of elements bonded using an adhesive with a notch situated on the interface. However in order to state such fact clearly it would be necessary to carry out additional experimental tests. Such tests should be planned so that actual fixing and loading conditions for the specimens are reflected in numerical modelling. The author shall try to carry out such tests and verify suitability of McClintock's hypothesis again in his next paper.

References

1. Ayatollahi M, Torabi A R. A criterion for brittle fracture in U-notched components under mixed mode loading. Engineering Fracture Mechanics 2009; 39: 1883–1896, https://doi.org/10.1016/j.engfracmech.2009.04.008.
2. Baranowski P, Damaziak K, Małachowski J. Brake system studies using numerical methods, Eksploatacja i Niezawodnosc – Maintenance and Reliability 2013; 15 (4): 337–342.
3. Bogy D B, Wang K C. Stress singularities at interface corners in bonded dissimilar isotropic elastic materials. International Journal of Solids and Structures 1971; 1: 993-1005, https://doi.org/10.1016/0020-7683(71)90077-1.
4. Byskov E. Calculation of stress intensity factors using finite element method with cracked elements. International Journal of Fracture Mechanics 1970; 6(2): 59-167, https://doi.org/10.1007/BF00189823.
5. Carpinteri A, Paggi M. Analytical study of the singularities arising at multi-material interfaces in 2D linear elastic problems. Engineering Fracture Mechanics 2007; 74: 59–74, https://doi.org/10.1016/j.engfracmech.2006.01.030.
6. Griffith A A. The phenomena of rupture and flow in solids. Philosophical Transactions series A 1920; 221: 163-198, https://doi.org/10.1098/rsta.1921.0006.
7. Kinloch A J. Adhesion and adhesives, Science and Technology. London: Springer, 1987, https://doi.org/10.1007/978-94-015-7764-9.
8. Kirsch G. Die theorie der elastizität und die bedürfnisse der festigkeitslehre. Verein deutscher Ingenieure Zeitschrift 1898; 29: 797-807.
9. Knesl Z, Klusak J, Nahlik L. Crack initiation criteria for singular stress concentrations, Part I: A Universal assessment of singular stress concentrations, Engineering Mechanics 2007; 14(6): 399–408.
10. Krishnan A, Xu L R. Systematic evaluation of bonding strengths and fracture toughnessess of adhesive joints. The Journal of Adhesion 2011; 87(1): 53–71, https://doi.org/10.1080/00218464.2011.538322.

11. Krishnan A, Xu LR. Experimental studies on the interaction among cracks, notches and interfaces of bonded polymers. International Journal of Solids and Structures 2013, 50: 1583–1596, https://doi.org/10.1016/j.ijsolstr.2013.01.024.

12. Krishnan A, Roy Xu L. An experimental study on the crack initiation from notches connected to interfaces of bonded bi-materials. Engineering Fracture Mechanics 2013; 111: 65–76, https://doi.org/10.1016/j.engfracmech.2013.08.010.

13. Leguillon D. A criterion for crack nucleation at a notch in homogeneous materials. Comptes Rendus de l'Académie des Sciences - Series IIB – Mechanics 2001; 329(2): 97–102, https://doi.org/10.1016/S1620-7742(01)01302-2.

14. Li Y, Song M. Method to calculate stress intensity factor of V-notch in bi-materials. Acta Mechanica Solida Sinica 2008; 21(4): 337–346, https://doi.org/10.1007/s10338-008-0840-3.

15. Łukaszewicz A. Nonlinear numerical model of heat generation in the rotary friction welding, Journal of Friction and Wear 2018; 39 (6): 612-619, https://doi.org/10.3103/S1068366618060089.

16. McClintock F A. Ductile fracture instability in shear. Journal of Applied Mechanics 1958; 25: 582-588.

17. Mieczkowski G. Description of stress fields and displacements at the tip of a rigid, flat inclusion located at interface using modified stress intensity factors. Mechanika 2015; 21(2): 91-98, https://doi.org/10.5755/j01.mech.21.2.8726.

18. Mieczkowski G. Stress fields and fracture prediction for adhesively bonded bi-material structure with sharp notch located on the interface. Mechanics of Composite Materials 2017; 53(3): 305-320, https://doi.org/10.1007/s11029-017-9663-y.

19. Mieczkowski G. Stress fields at the tip of a sharp inclusion on the interface. Mechanics of Composite Materials 2016; 52(5):601-610, https://doi.org/10.1007/s11029-016-9610-3.

20. Naik R A, Crews J H. Determination of stress intensity factors for interface cracks under mixed-mode loading. Paper presented at the ASTM National Symposium on Fracture Mechanics, June 30-July 2,1992, Gatlinburg, TN.

21. Parton V ., Perlin P I. Mathematical methods of the theory of elasticity. Moscow: Mir Publishers, 1984.

22. Pirondi A, Nicoletto G. Fatigue crack growth in bonded DCB specimens. Engineering Fracture Mechanics 2004; 71(4–6): 859–871, https://doi.org/10.1016/S0013-7944(03)00046-8.

23. Ritchie R O, Knott J F, Rice J R. On the relation between critical tensile stress and fracture toughness in mild steel. Journal of the Mechanics and Physics of Solids 1973; 21: 395-410, https://doi.org/10.1016/0022-5096(73)90008-2.

24. Rogowski G, Molski K L. The T-stress effect on the plastic zone size in a thin ductile material layer sandwiched between two elastic adherents. Engineering Fracture Mechanics 2016; 168 (A): 260-270.

25. Rudawska A, Dębski H. Experimental and numerical analysis of adhesively bonded aluminium alloy sheets joints. Eksploatacja i Niezawodnosc – Maintenance and Reliability 2011; 1: 4–10.

26. Savruk M P, Shkarayev S, Madenci E. Stress near apex of dissimilar material with bilinear behavior. Journal of Applied Fracture Mechanics 1999; 31: 203-212, https://doi.org/10.1016/S0167-8442(99)00014-2.

27. Seweryn A, Łukaszewicz A. Verification of fracture criteria of elements with V-shaped notches. Eksploatacja i Niezawodnosc — Maintenance and Reliability 2001; 5: 6–8.

28. Seweryn A, Molski K. Elastic stress singularities and corresponding generalized stress intensity factors for angular corners under various boundary conditions. Engineering Fracture Mechanics 1996; 55: 529-556, https://doi.org/10.1016/S0013-7944(96)00035-5.

29. Sih G C. Strain-energy-density factor applied to mixed mode crack problems. International Journal of Fracture 1974; 10: 305-321, https://doi.org/10.1007/BF00035493.

30. Sih G C, Chen E P. Cracks in composite materials, Ch.3 (Mechanics of Fracture VI) ed. G. C. Sih. Hague: Martinus Nijhoff Publishers, 1981.

31. Sneddon I N. The distribution of stress in the neighbourhood of a crack in an elastic solid. Proceedings of the Royal Society of London A 1946;187(1009): 229-260, https://doi.org/10.1098/rspa.1946.0077.

32. Sun C T, Jih C J. On strain energy release rates for interfacial cracks in bi-material media. Engineering Fracture Mechanics 1987; 28: 13-20, https://doi.org/10.1016/0013-7944(87)90115-9.

33. Sun C T, Qian H. Brittle fracture beyond the stress intensity factor. Journal of Mechanics of Materials and Structures 2009; 4(4): 743-753, https://doi.org/10.2140/jomms.2009.4.743.

34. Taylor, D. The Theory of Critical Distances: A new perspective in fracture mechanics. Oxford: Elsevier, 2007.

35. Tracey D M. Finite elements for determination of crack tip elastic stress intensity factors. Engineering Fracture Mechanics 1971; 3(3): 255-265, https://doi.org/10.1016/0013-7944(71)90036-1.

36. Tran V-X, Leguillon D, Krishnan A. Interface crack initiation at V-notches along adhesive bonding in weakly bonded polymers subjected to mixed-mode loading. International Journal of Fracture Mechanics 2012; 176: 65–79, https://doi.org/10.1007/s10704-012-9727-x.

37. Treifi M, Oyadiji S O. Strain energy approach to compute stress intensity factors for isotropic homogeneous and bi-material V-notches. International Journal of Solids and Structures 2013; 50: 2196–2212, https://doi.org/10.1016/j.ijsolstr.2013.03.011.

38. Williams M L. Stress singularities resulting from various boundary conditions in angular corners of plate in extension. Journal of Applied Mechanics 1952; 9: 526-528

Grzegorz MIECZKOWSKI
Faculty of Mechanical Engineering
Bialystok University of Technology
ul. Wiejska 45C, Poland

E-mail: g.mieczkowski@pb.edu.pl